Geophysical Prospecting, 1998, **46**, 423–440

Multiple prediction using the homeomorphic-imaging technique[1]

Shemer Keydar,[2] Evgeny Landa,[2] Boris Gelchinsky[3] and Igor Belfer[2]

Abstract

A new method for predicting different kinds of multiples and peg-leg reflections in unstacked seismic data is discussed. The basis for this method is the fact that kinematic properties of multiples can be represented as a combination of kinematic properties of primary reflections. The prediction is made using a two-step process. In the first step, the values for the angle of emergence and radius of curvature of the wavefront for primary reflections from 'multiple-generating' interfaces are obtained. These parameters are estimated directly from unstacked data for every source point using the homeomorphic-imaging technique. The second step consists of prediction of multiples from primary reflections that satisfy a so-called 'multiple condition'. This condition is the equality of the absolute values of the angles of emergence calculated from the first step. This method is effective even in complex media and information on the subsurface geology is not required. The parameters are estimated directly from the unstacked data and do not require any computational efforts such as in wavefield extrapolation of data.

Introduction

Multiple-suppression techniques make use of the different characteristics that distinguish multiple from primary reflections. The characteristics most frequently used are the moveout difference between multiple and primary and the periodic nature of multiples due to the fact that multiples are repetitions of some primary reflection. The first characteristic may be exploited to attenuate the multiples by stacking the data (Schneider, Prince and Giles 1965) or moveout filters (Hardy, Warner and Hobbs 1989; Yilmaz 1989). Short-period multiples are approximately periodic and may be discriminated using predictive and adaptive deconvolution methods (Backus 1959; Peacock and Treitel 1969; Griffiths, Smolka and Trembly 1977). Another common approach is suppression based upon wave-equation methods (Berryhill and Kim 1986; Wiggins 1988; Fokkema and Van den Berg 1990; Verschuur and Berkhout 1992). The wave-equation methods produce a model of water-bottom peg-leg multiples by extrapolating the recorded data through the water layer and subtracting it from the

[1] Received May 1997, revision accepted February 1998.
[2] The Geophysical Institute of Israel, PO Box 2286, Holon 58122, Israel.
[3] Department of Geophysics, Tel-Aviv University, Ramat Aviv, Israel.

data. The traveltime through the water layer is required to produce an accurate time prediction and an estimate of the water-bottom reflectivity function is required to calculate multiple amplitudes.

Not all the proposed approaches lead to a 'panacea solution' for multiple attenuation. Even the most powerful and comprehensive methods cannot remove all types of multiples. We introduce a new target-orientated approach to predict kinematic properties of any kind of multiple for a given primary reflection from 'multiple-generating' interfaces. Unlike wave-equation extrapolation methods, it does not require any *a priori* knowledge of the subsurface geology or waveform information and does not require significant computational effort to perform the wavefield extrapolation of prestack seismic data. The concept of this approach is explained in the following sections and the method is demonstrated using both synthetic and field examples.

Basics (Geometrical considerations)

We describe here the main basic concepts of the method. Figure 1 depicts three reflectors n, $n-1$ and $n-2$ beneath an arbitrary overburden. A raypath $A_sC_1C_2C_3A_k$ C_4A_r of the interlayer peg-leg multiple is shown connecting one source A_s with one receiver A_r. We can see that the arrival time of this kind of multiple can be represented as a combination of four primary reflections; from reflector n, $n-1$ and two reflections from reflector $n-2$. From the above, the arrival time for the interlayer peg-leg multiple

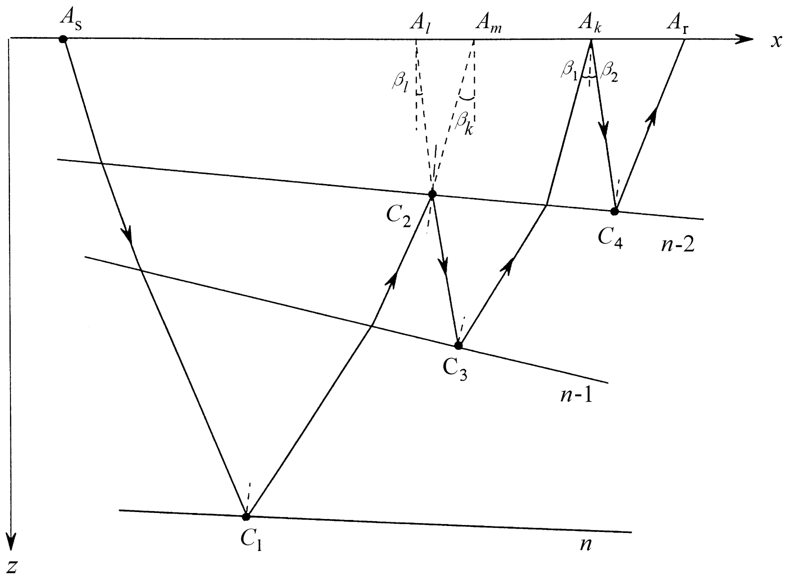

Figure 1. Ray scheme for an interlayer peg-leg multiple event $A_sC_1C_2C_3A_kC_4A_r$. The arrival time of this multiple is a simple combination of arrival times of the primary reflections, namely $A_sC_1A_m$, $A_mC_2A_l$, $A_lC_3A_k$ and $A_kC_4A_r$.

can be given by

$$T_{sr}^{n(n-1)(n-2)} = T_{sm}^{n} + T_{kl}^{n-1} - T_{lm}^{n-2} + T_{kr}^{n-2}, \tag{1}$$

where T_{sm}^{n} is the traveltime of waves reflected from interface n with the source at A_s and receiver A_m; T_{kl}^{n-1} is the traveltime of waves reflected from interface $n-1$ with the source at A_k and receiver A_l; T_{lm}^{n-2} is the traveltime of waves reflected from interface $n-2$ with the source at A_l and receiver A_m; and T_{kr}^{n-2} is the traveltime of waves reflected from interface $n-2$ with the source at A_k and receiver at A_r. When the order of multiple increases by one, it gives rise to an additional reflection. In general it can be shown that any multiples of any order can be represented as a combination of primary reflections.

Multiple condition

We can now formulate conditions for multiple prediction for interlayer peg-leg multiples. From Fig. 1, it is evident that the angle of emergence of the wavefront of the primary reflection $A_sC_1A_m$ from reflector n is equal to the angle of emergence of the primary reflection $A_lC_2A_m$ from reflector $n-2$, the angle of emergence of primary reflection $A_kC_3A_l$ from reflector $n-1$ is equal to the angle of emergence of primary reflector $A_mC_2A_l$ from reflector $n-2$, and from Snell's law it stems that the angle of emergence of the wavefront of primary reflection $A_lC_3A_k$ from reflector $n-1$ is equal to the angle of emergence of primary reflection $A_rC_4A_k$ from reflector $n-2$. These conditions can be expressed in the following equations:

$$\begin{aligned} \beta_{sm}^{n} &= \beta_{lm}^{n-2}, \\ \beta_{kl}^{n-1} &= \beta_{ml}^{n-2}, \\ \beta_{lk}^{n-1} &= \beta_{rk}^{n-2}, \end{aligned} \tag{2}$$

where β is the angle of emergence of the wavefront, the upper index denotes the number of the reflector, the first bottom index denotes the location of the shot and the second the location of the receiver.

We shall refer to expressions (2) as a 'multiple condition'.

Prediction procedure

For a given type of multiple, the procedure of multiple predictions consists of the following steps:

1 The angle of emergence and radius of curvature for every offset (receiver position) of the wavefront of the primary reflection from multiple-generating interfaces are obtained for each common-shot gather.

2 For a given source-receiver location all possible primary reflections that satisfy the multiple condition are selected (thereby defining the points A_l, A_m and A_k in Fig. 1).

3 Calculation of the arrival times for a given source-receiver location from primary reflections.

The crucial step in our prediction method is the derivation of the angle of emergence of the wavefront of a given primary reflection for each shot at every receiver location. Several algorithms have been suggested for this purpose (Shultz and Claerbout 1978; Biondi 1992). They all calculate the angle of emergence (or p-parameter) using zero-offset arrival times and the stacking velocity. Such a calculation usually requires numerical differentiation procedures which are very sensitive to errors in estimated parameters. We estimate these parameters directly from unstacked data using the common-shot homeomorphic-imaging (HI) method. It requires no more than that the near-surface values of the velocity field be known.

The concept of this method is explained briefly in the following section.

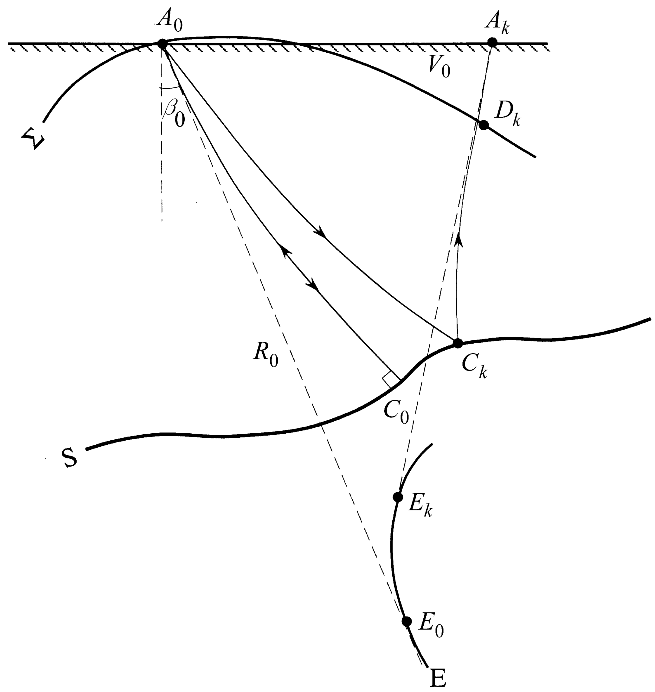

Figure 2. Ray diagram for estimating the angle of emergence and radius of wavefront curvature. From a source located at A_0, two rays are emitted in a 2D inhomogeneous model. The first is a normal ray $A_0C_0A_0$ and the second a ray $A_0C_kA_k$ emerging at the receiver located at A_k. The common-shot wavefront Σ emerges at the point A_0 under the angle β_0. The radius of curvature of this wavefront is R_0. The true subsurface model is substituted by an effective model consisting of a homogeneous half-space with velocity V_0. The wavefront Σ is then approximated in the vicinity of A_0 by an effective wavefront with the same radius of curvature R_0 and the same angle of emergence β_0. The locus of centres of curvature of the effective wavefront is E.

Common-shot homeomorphic-imaging method

The estimated angle of emergence and radius of curvature of the wavefront of primary reflections are based on measuring the coherence of a common shot (common-receiver gather) using the common-shotpoint (CSP) HI method (Gelchinsky 1989; Keydar, Gelchinsky and Berkovitch 1996). The basis of the CSP HI method is a new local moveout time correction. As indicated above, the CSP HI method does not require a knowledge of the overburden. All that is needed, even for a laterally inhomogeneous true subsurface model, is the near-surface velocity V_0, assumed to be known already and constant in the vicinity of each source-point location.

Figure 2 shows the basic ray diagram of the CSP method.

Let us assume that a normal incident ray is emitted at source point A_0, reflected from an interface S at point C_0 and emerges at A_0 (Fig. 2) at time t_0. Let us further assume that another ray emitted at source A_0 is reflected from the interface S and emerges at

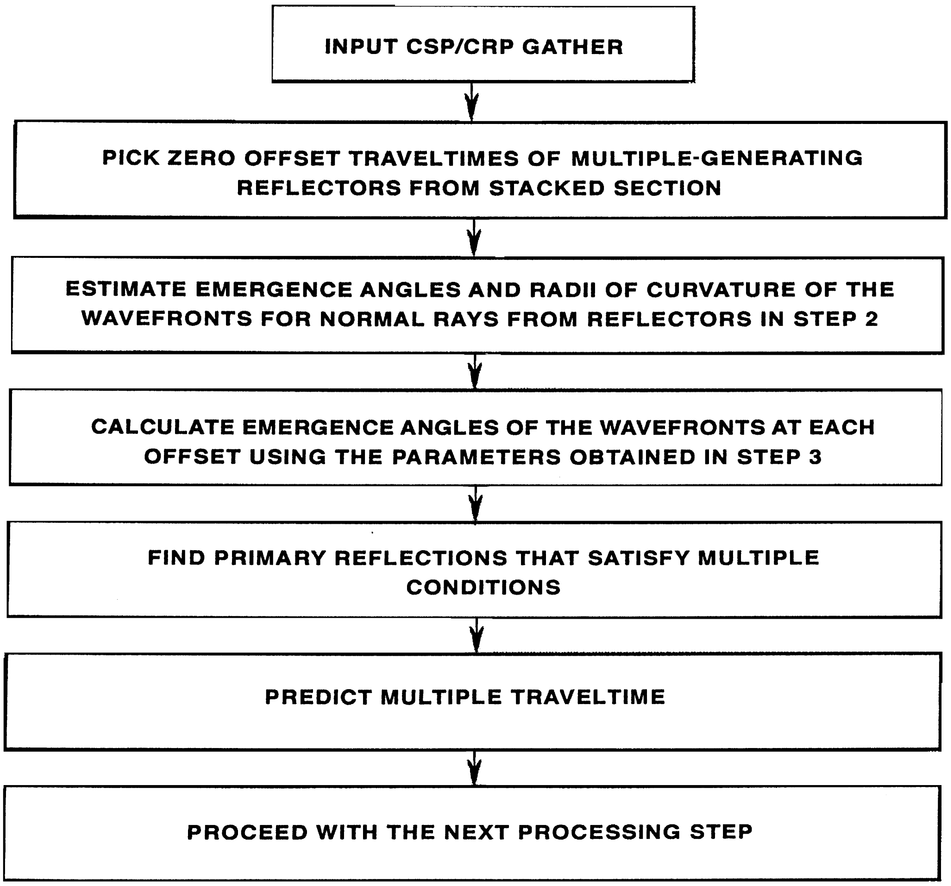

Figure 3. A flow chart of the proposed prediction procedure.

point A_k at time t_k. We denote the angle of emergence of the normal ray at A_0 by β_0 and the radius of the CS wavefront at A_0 by R_0.

One of the key ideas of the CSP HI method is to substitute the laterally inhomogeneous true subsurface model by the effective model. This consists, in respect of the CS gather at A_0, of a homogeneous half-space. We then assume that the true CS wavefront, Σ, is approximated in the vicinity of A_0 by an effective wavefront with the same radius of curvature, R_0, and the same angle of emergence, β_0. The effective wavefront relates to propagation in the effective medium with its evolute (locus of the centres of curvature of the wavefront) at E surrounding point E_0. The element E is called a homeomorphic image of the element of reflector C_0C_k. The total set of images on the continuum of central points A_0 constructs an effective reflector that corresponds to reflector S. The time correction $\Delta\tau_k$ for the arbitrary kth trace corresponding to a source A_0 and receiver A_k is described by the relationship,

$$\Delta\tau_k = \tau(A_0C_kA_k) - \tau(A_0C_0A_0) = D_kA_k/V_0, \qquad (3)$$

where V_0 is the velocity at the reference level, constant in the vicinity of A_0; $A_0C_kA_k$ is the travelpath from source A_0 to receiver A_k; D_kA_k is the difference in travelpath between zero-offset trace A_0C_0 and the kth trace $A_0C_kA_k$. By choosing a different order of approximation for the front caustic E_0, various parametrized relationships for the segment D_kA_k can be obtained. The order of approximation depends on the distance between the central point location and the furthest receiver. If A_0A_k is large, the approximation fails. For a wide class of models and moderate offsets, the wavefront element can be approximated as the arc of a circle. This means that the caustic of the front shrinks to a point and, in such a case, the angle of emergence β_0 of the normal emergence ray A_0C_0 and the radius of wavefront curvature R_0 at point A_0 can be used

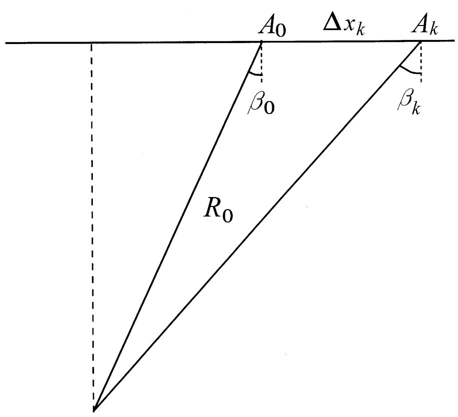

Figure 4. Using the estimated angles of emergence β_0 and radii of curvature R_0 of the wavefront for normal incidence, we use a simple relationship (5) to obtain the angle of emergence β_k for different receiver positions. Δx_k is the offset distance between the zero-offset located at A_0 and a receiver located at A_k.

to compute the local NMO correction. Assuming a circular wavefront and a locally flat recording plane the following simple relationship is obtained:

$$\Delta\tau_k = \sqrt{R_0^2 + 2R_0\Delta x \sin\beta_0 + \Delta x^2} - R_0/V_0, \tag{4}$$

where Δx is the distance between source A_0 and receiver A_k. The unknown parameters, the angle of emergence β_0 and radius of curvature R_0, can be estimated using the wave-correlation procedure (Taner and Koehler 1969; Gelchinsky, Landa and Shtivelman 1985). The search is performed around the zero-offset time of a specified primary reflection (interpreted from a stacked section). The near-surface velocity V_0 should either be known or can be one of the search parameters. Semblance maximization is carried out using an optimization algorithm. Time correction is applied for each central trace located at the source location.

Implementation

According to the scheme described above, the method for prediction of multiples is implemented as follows (Fig. 3):

Once the angles of emergence and the radii for normal incidence of the wavefront

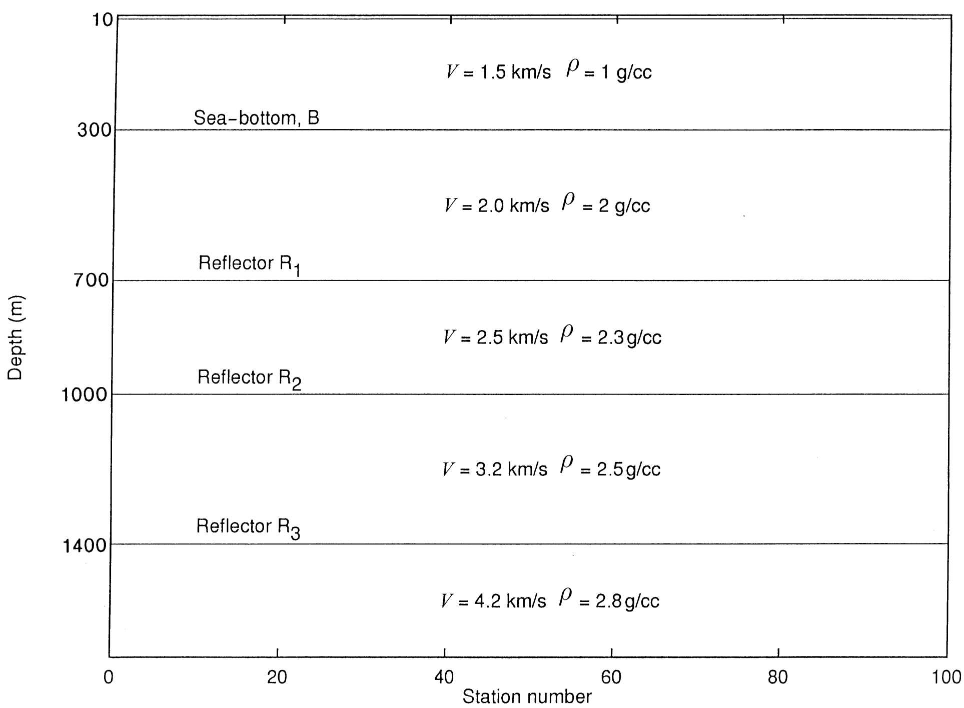

Figure 5. A simple five-layer shallow water model (after Zhou and Greenhalgh 1996).

have been estimated for all shot positions, we can obtain the angle of emergence for different receiver positions (offset) from the shot using the following expression (Fig. 4):

$$\sin\beta = \frac{\Delta x + R_0 \sin\beta_0}{\sqrt{R_0^2 + 2R_0 \sin\beta_0 \Delta x + \Delta x^2}}. \tag{5}$$

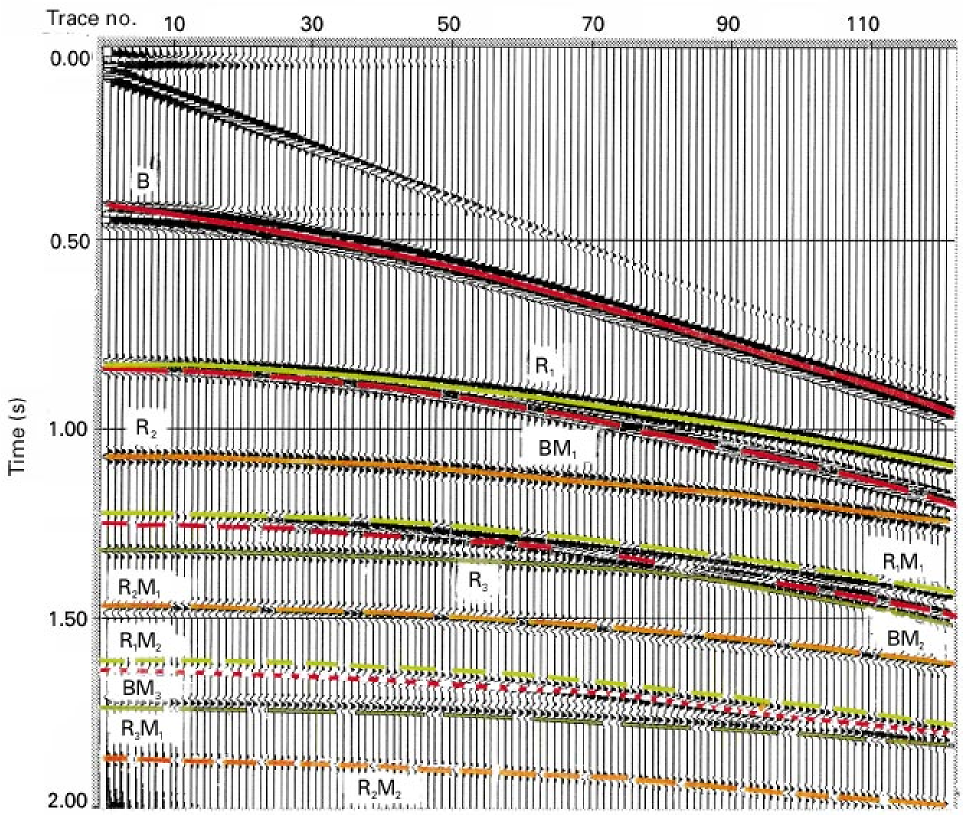

Figure 6. The synthetic CSP gather created for the model in Fig. 5 using acoustic modelling. The primary reflections from B (the sea-bottom), R_1, R_2 and R_3 are labelled on the section. The water-layer reverberations corresponding to the reflector B are BM_1, BM_2, BM_3, the first-, second- and third-order surface multiples, respectively. The symbols R_1M_1, R_1M_2 on the seismic section stand for the first- and second-order peg-leg multiples from reflector R_1. The peg-leg multiples from reflector R_2 are R_2M_1 and R_2M_2. Only the first-order multiple R_3M_1 from reflector R_3 can be observed. Primaries are indicated by solid lines and multiples by dashed lines. As the order increases, so the dashes become smaller. The primary reflections from B and multiples corresponding to this reflector are shown in red. Primary reflections from R_1 and its multiples are shown in green; primary reflections from R_2 and its multiples are shown in orange and the primary reflections from R_3 and corresponding multiples are shown in dark green.

Thus, for a given source receiver, using these angles of emergence, we can define the locations of points which satisfy the multiple condition (points $A_k A_l$ and A_m in Fig. 1). This can be achieved by scanning all possible locations. The traveltime of the multiple reflection for the given source receiver can now be predicted using (1) for interlayer peg-leg multiples. The arrival time of the primary reflection for a source located at A_0 from reflector n and for a receiver located at A_k is calculated using (4) and the zero-offset arrival time for this source. From the above, the following expression for an interlayer peg-leg multiple is obtained:

$$\begin{aligned} T_{sr}^{n(n-1)(n-2)} &= T_{sm}^{n} + T_{kl}^{n-1} - T_{lm}^{n-2} + T_{kr}^{n-2} \\ &= T_{s0}^{n} + \Delta\tau_{sm}^{n} + T_{k0}^{n-1} + \Delta\tau_{kl}^{n-1} - T_{l0}^{n-2} - \Delta\tau_{lm}^{n-2} + T_{k0}^{n-2} + \Delta\tau_{kr}^{n-2}, \end{aligned} \tag{6}$$

where T_{s0}^{n}, T_{k0}^{n-1}, T_{l0}^{n-2} and T_{k0}^{n-2} are the zero times for points A_s, A_k, A_l for reflectors n, $n-1$ and $n-2$; $\Delta\tau_{sm}^{n}$ is the time correction for shot A_s and receiver A_m for reflector n; $\Delta\tau_{kl}^{n-1}$ is the time correction for shot A_k and receiver A_l for reflector $n-1$; τ_{lm}^{n-2} is the time correction for shot A_l and receiver A_m for reflector $n-2$; $\Delta\tau_{kr}^{n-2}$ is the time correction for shot A_k and receiver A_r for reflector $n-2$. (The first bottom index denotes the location of the shot, the second the location of the receiver and the upper index is the number of the reflector.)

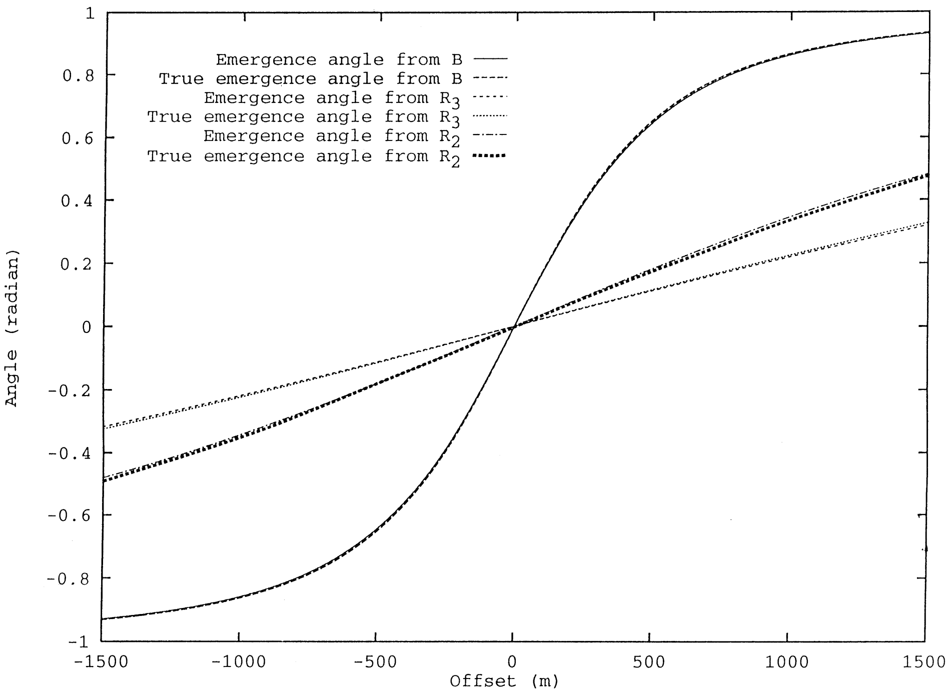

Figure 7. Angle of emergence of wavefronts for the sea-bottom B, and the second and third reflectors, R_2 and R_3, as a function of offsets obtained using (6).

Synthetic examples

A five-layer shallow water model described by Zhou and Greenhalgh 1996) was used to test our method of multiple prediction (Fig. 5). A CSP record was calculated using acoustic modelling (Schmidt and Tango 1986) (Fig. 6). The distance between receivers was 10 m and the sampling rate was 4 ms. The identification of waves is given in the caption. The CSP HI procedure for analysing the normal rays was applied for the sea-bottom and three reflectors. The angles of emergence of the wavefronts at zero-offset were equal to zero degrees and the estimated values of the radii of curvature of the wavefronts from the bottom, second and third reflectors had an error of less than 4%. Figure 7 is the extrapolated angle of emergence of wavefronts from the bottom, second and third reflectors for different offsets. We can see that the values extrapolated essentially coincide with the true values.

A surprising result was obtained for the first reflector. The error in the estimated radius of curvature was about 25%. Testing the CSP record (Fig. 6), we noted that the source of the error is contamination by the first-order multiple (BM_1), which has the same zero-offset time as the primary from the first reflector. An acceptable error of less

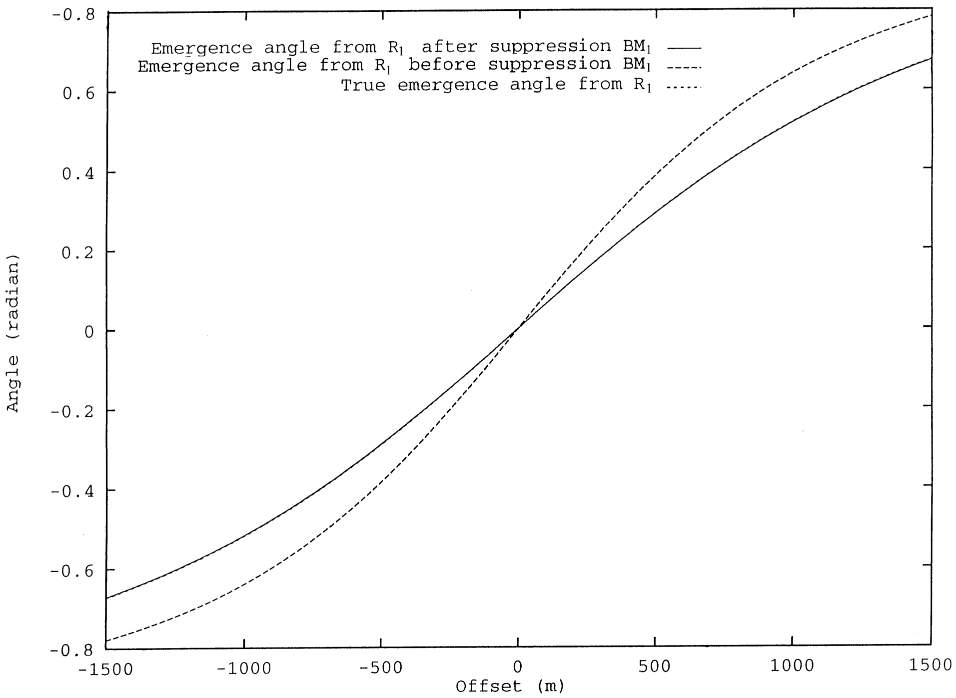

Figure 8. Angle of emergence of the wavefront for the first reflector obtained using the radius of curvature of the wavefront at zero-offset before sea-bottom suppression (long-dash line) and after sea-bottom suppression (solid line). The actual angle of emergence is indicated by the short-dash line.

than 3% on the radius of curvature for the first reflector was only obtained after applying a $\tau - p$ multiple suppression filter, using predicted traveltimes for sea-bottom multiple (BM_1), to remove contamination of the primary event (R_1) by the sea-bottom multiple (BM_1). In general, where ambiguity exists between a primary and a multiple, which is some form of conventional multiple, suppression may be applied prior to the application of the proposed prediction procedure. Although there is interference between reflector R_3 and the sea-bottom multiple BM_2, the error in the estimated radius is good (less than 3%) owing to the fact that the zero-offset times of both events are different.

The extrapolated angles of emergence for the first reflector before and after bottom-multiple suppression are shown in Fig. 8. Using the angles of emergence of primary reflections and satisfying the multiple condition, arrival times of sea-bottom multiples, multiples from the first reflector, multiples from the second reflector and multiples from the third reflector were obtained (Fig. 6, dashed coloured lines). Now, from the predicted traveltimes, the multiple model can be constructed followed by multiple subtraction (Zhou and Greenhalgh 1996; Landa, Belfer and Keydar, submitted to *Geophysics*).

In order to demonstrate the generality of the proposed prediction procedure, a more complex model including a dipping sea-bottom with a dipping basalt horizon was used

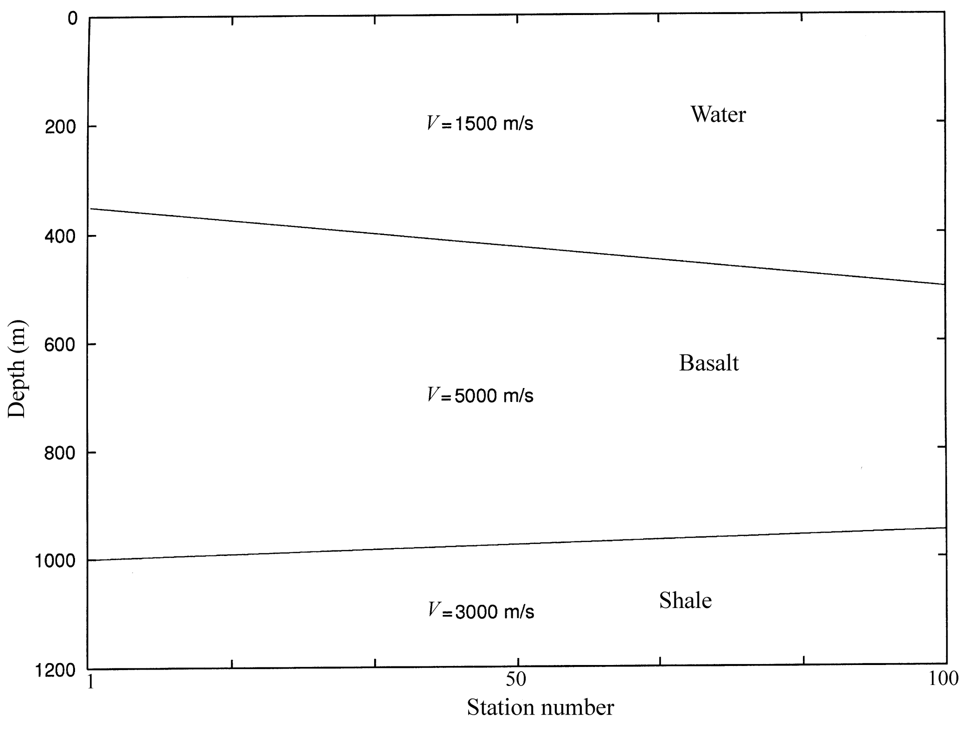

Figure 9. Model with dipping sea-bottom and dipping basalt horizon.

(Fig. 9). A total of 100 common-shot records were calculated using full-wave equation modelling. Each common-shot gather consists of 48 receivers. The distance between receivers was 40 m, the same as the distance between sources. The minimum offset was 40 m. The sampling rate was 2 ms.

A typical CSP gather is shown in Fig. 10. The reflected wave from the sea-bottom appears at a zero time of about 0.4 s, and the reflection from the basalt layer appears at 0.7 s. The aim of this example is to predict the first- and second-order sea-bottom multiples and the first- and second-order peg-leg multiples from the basalt horizon. In order to perform the prediction, the CSP HI method was applied along zero-offset times of the first and second reflectors to estimate the angles of emergence and radii of wavefronts from these reflectors. The results of estimated radii of wavefront curvature from the first and second layers are shown in Fig. 11. The rms errors in angle

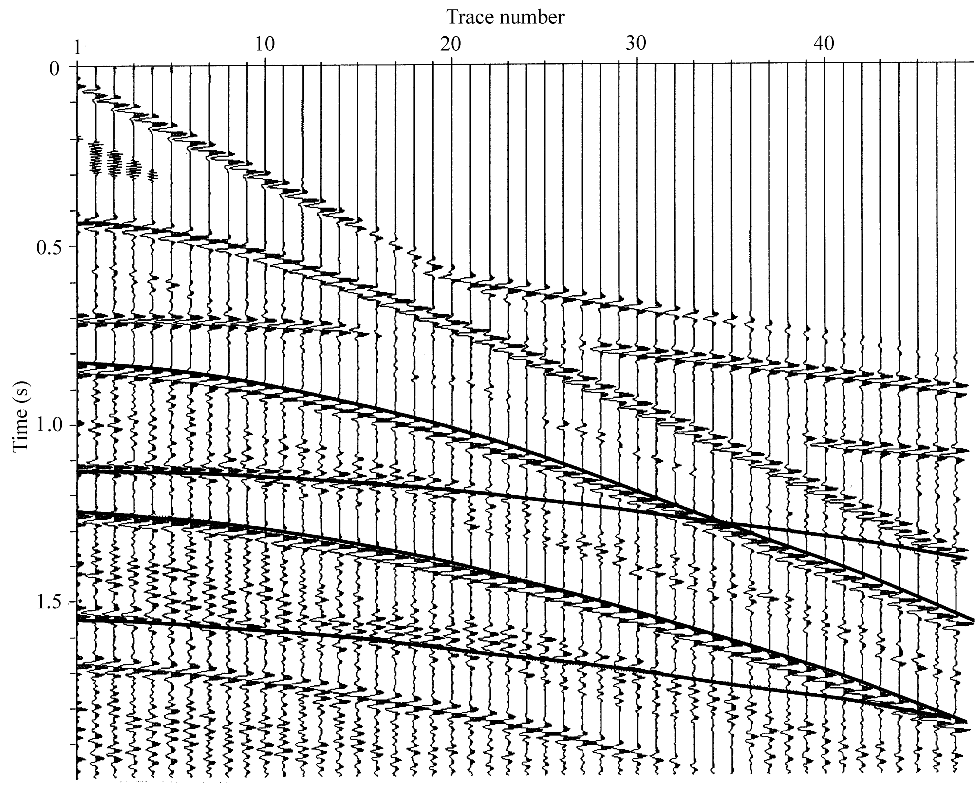

Figure 10. CSP gather generated for the model (Fig. 9) using full-wave equation modelling. The primary reflected wave from the sea-bottom appears at about 0.4 s and the primary reflected wave from the basalt horizon appears at 0.7 s. The predicted arrival times of the first-order surface multiple at about 0.8 s, the second-order surface multiple at about 1.2 s, the first-order peg-leg multiple from the basalt horizon at about 1.1 s and the second-order peg-leg multiple from the basalt horizon at about 1.5 s are indicated by solid lines.

estimation for both layers were less than 1%. The rms errors in radii estimation were about 3%.

In the next step the angles of emergence for normal rays were extrapolated at every offset using (5). Finally the traveltimes of multiples were calculated from the primary reflections that satisfy the multiple conditions. The predicted arrival times of four multiples (two sea-bottom and two peg-leg) from the basalt horizon are shown in Fig. 10 by solid lines. A good fit between the predicted times and those calculated by modelling can be observed.

Real data example

The multiple prediction procedure was applied to a marine seismic line. The data were recorded using a 120-channel hydrophone streamer with a 25 m group interval and minimum offset of 139 m. The data were recorded at a 4 ms sampling rate. The first water-layer reverberation is visible at about 0.8 s on a conventional data stack (Fig. 12). The other water peg-leg multiple of the first order from reflector M (about 1.8 s) is present at about 2.2 ms. For this data set, we apply our multiple prediction procedure to predict multiple arrivals of the first water-layer reverberation and first-order peg-leg

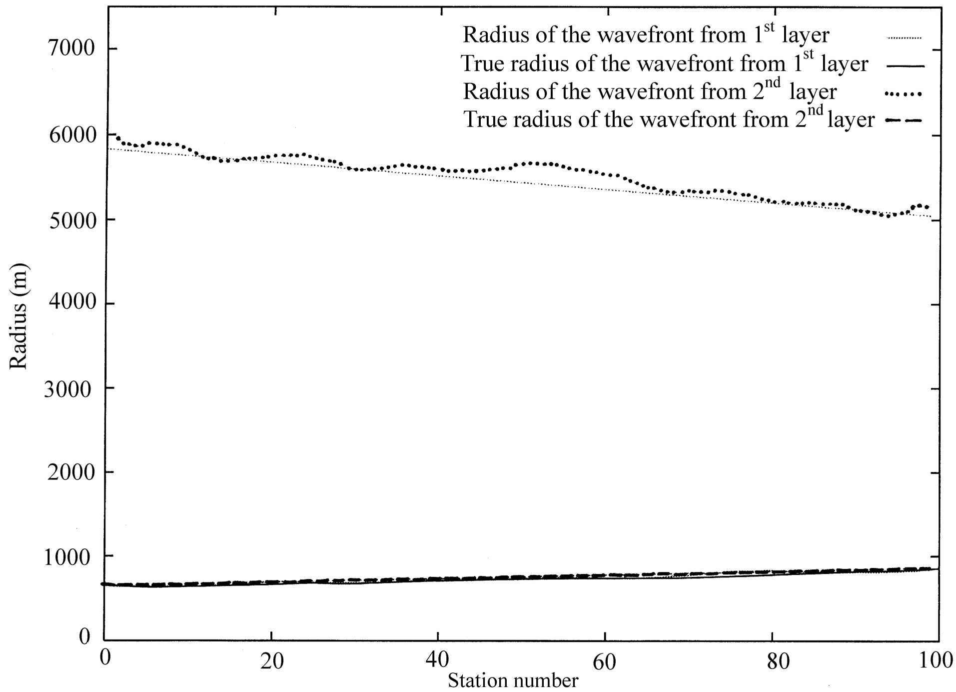

Figure 11. The estimated and actual radii of curvature of the wavefront from the first layer (dashed and solid lines) and the second layer (small and large dots).

multiples from reflector M (1.8 s). For this purpose the angles of emergence and radii of curvature of the wavefront from the sea-bottom and reflector M were obtained using our procedure. the radii and angles of emergence for the sea-bottom are shown in Figs 13(a,b) and the radii and angles of emergence for reflector M are shown in Figs 14(a,b). The predicted zero-offset times of the first sea-bottom multiple and a strong multiple produced by reflector M are shown in Fig. 12 by solid lines. Figure 15 shows a CMP gather with the predicted traveltimes of the sea-bottom and peg-leg multiples indicated by solid lines.

Conclusions

A new method for predicting kinematic properties of different kinds of multiples and peg-leg reflections in unstacked seismic data is proposed. The method is based on the homeomorphic-imaging (HI) technique. The prediction is made using a two-step process. In the first step, the values for the angle of emergence and radii of curvature of the wavefront for primary reflections from multiple-generating interfaces are obtained;

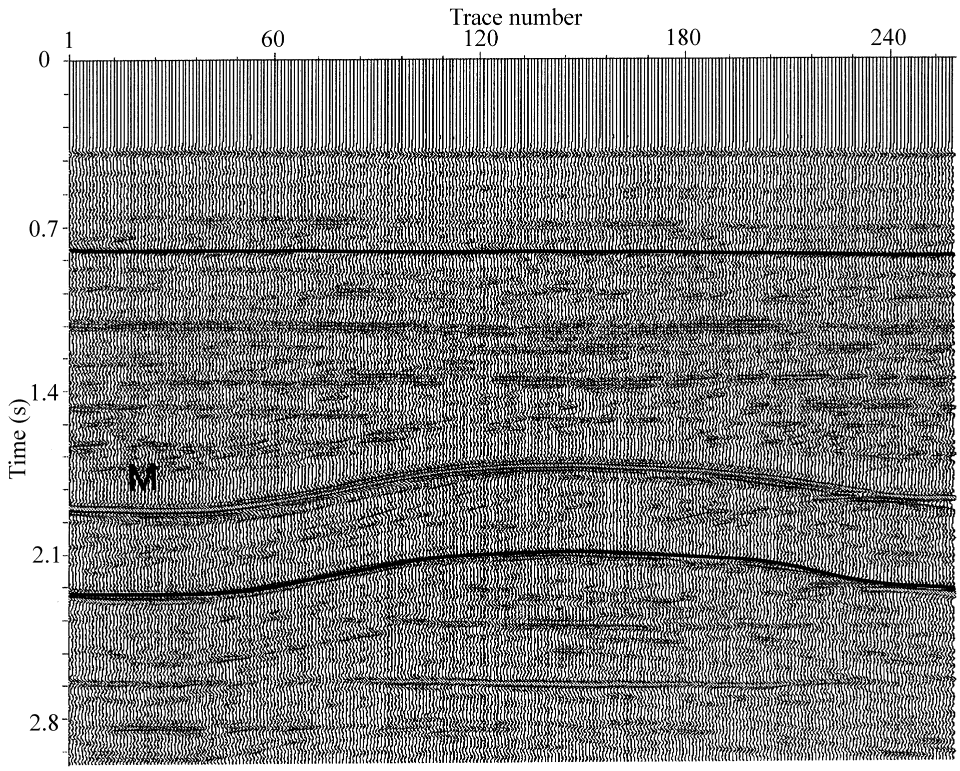

Figure 12. A stacked section of real marine data. The predicted zero-offset times of the first surface multiple and a strong peg-leg from the reflector M are indicated by solid lines.

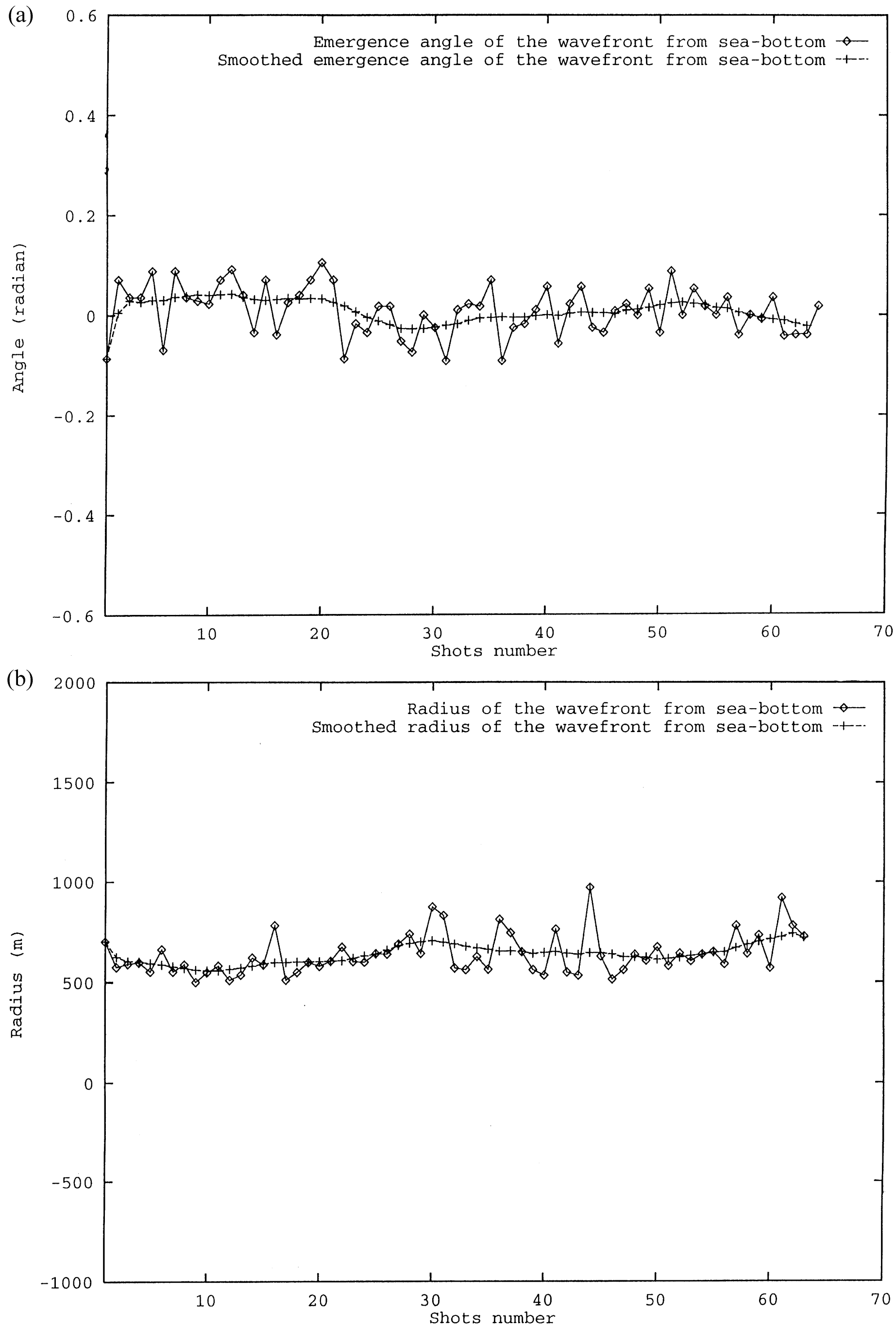

Figure 13. (a) Estimated angle of emergence of the wavefront for reflection from the sea-bottom with and without smoothing. (b) Estimated radius of curvature of the wavefront for reflection from the sea-bottom with and without smoothing.

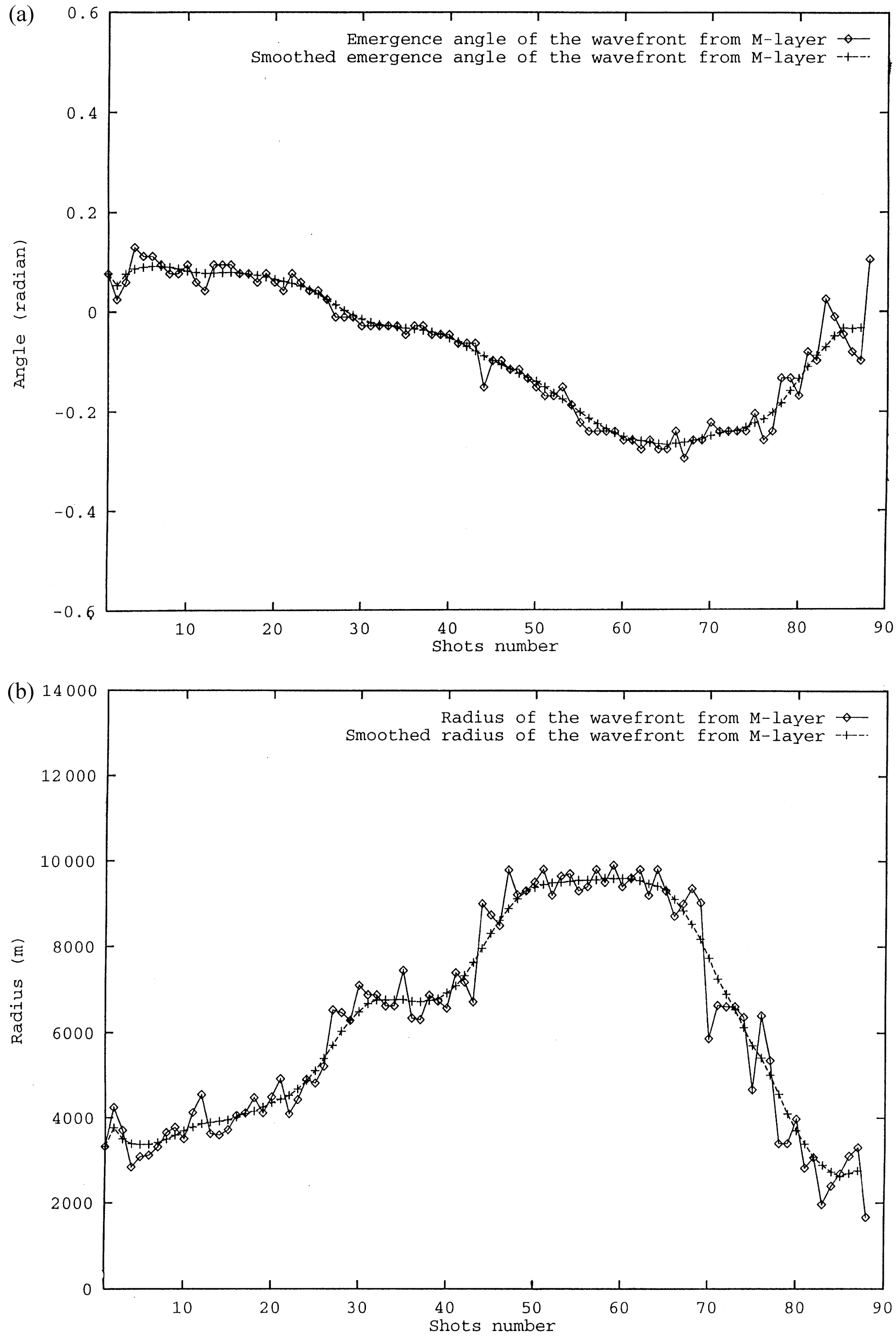

Figure 14. (a) Estimated angle of emergence of the wavefront from reflector M with and without smoothing. (b) Estimated radius of curvature of the wavefront from reflector M with and without smoothing.

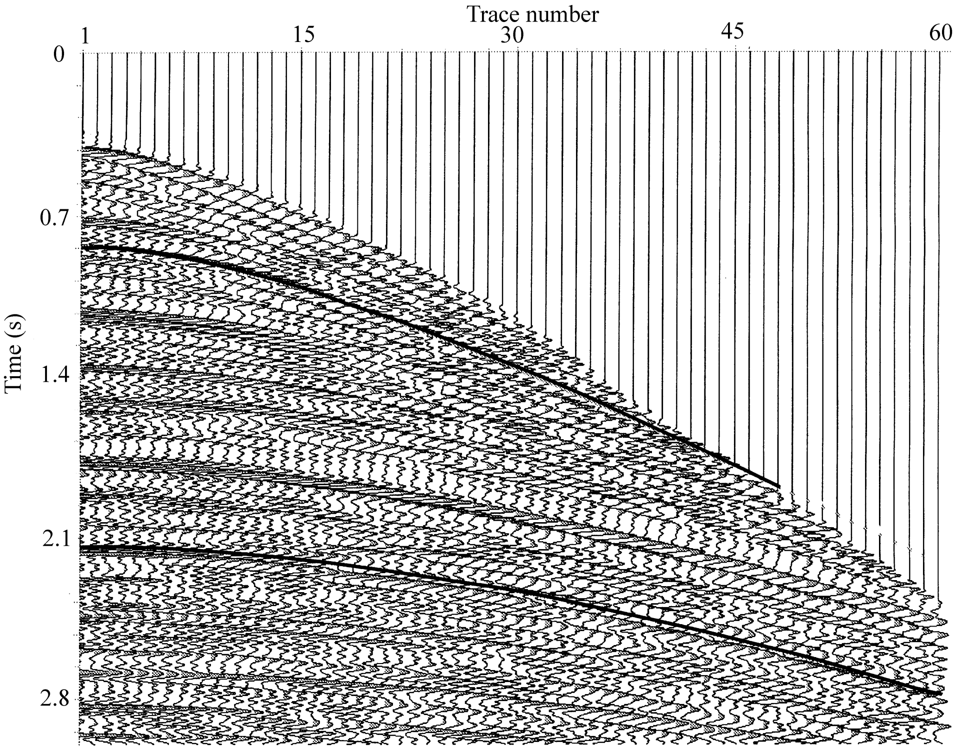

Figure 15. The CMP gather. Predicted traveltimes for the first-order surface multiple at about 0.8 s and first-order peg-leg multiples at about 2.1 s are indicated by solid lines.

these parameters are estimated for every source point directly from unstacked data using the HI technique. The second step consists of multiple prediction from primary reflectors that satisfy the so-called multiple condition; this condition is the equality of the absolute values of the angles of emergence calculated from the first step.

The main advantages of the proposed method are:

1 No information on subsurface geology is required.

2 The proposed method is equally valid for all types of multiples (water-bottom, peg-leg and interbed), provided it is possible to pick primaries from multiple-generating interfaces on a CMP stack section.

The synthetic and numerical examples given demonstrate the power of the proposed method.

Acknowledgements

This work was sponsored by the Earth Science Research Administration of the Israel Ministry of National Infrastructures. The authors would like to thank Debbie Artzi for editing the manuscript. We wish to thank Dr Hobbs and two anonymous reviewers for their review of this paper and their constructive comments.

References

Backus M.M. 1959. Water reverberations, their nature and elimination. *Geophysics* **55**, 1508–1511.

Berryhill J.R. and Kim Y.C. 1986. Deep water peg-legs and multiples: emulation and suppression. *Geophysics* **51**, 2177–2184.

Biondi B. 1992. Velocity estimation by beam stack. *Geophysics* **57**, 1034–1047.

Fokkema J. and Van den Berg P. 1990. Removal of surface-related wave phenomena: the marine case. 60th SEG meeting, San Francisco, USA, Expanded Abstracts, 1689–1692.

Gelchinsky B. 1989. Homeomorphic imaging in processing and interpretation of seismic data (fundamentals and schemes). 59th SEG meeting, Dallas, USA, Expanded Abstracts, 983–988.

Gelchinsky B., Landa E. and Shtivelman V. 1985. Algorithms of phase and group correlation. *Geophysics* **50**, 596–608.

Griffiths L.J., Smolka F.I. and Trembly L.D. 1977. Adaptive deconvolution: a new technique for processing time-varying seismic data. *Geophysics* **42**, 742–759.

Hardy R.J.J., Warner M.R. and Hobbs R.W. 1989. Labeling long-period multiple reflections. *Geophysics* **54**, 122–126.

Keydar S., Gelchinsky B. and Berkovitch A. 1996. Common shot-point stacking and imaging method. *Journal of Seismic Exploration* **5**, 261–274.

Peacock K. and Treitel S. 1969. Predictive deconvolution – theory and practice. *Geophysics* **34**, 155–169.

Schmidt M. and Tango G. 1986. Efficient global matrix approach to the computation of synthetic seismograms. *Geophysical Journal of the Royal Astronomical Society* **86**, 331–359.

Schneider W., Prince E. and Giles B. 1965. A new data-processing technique for multiple attenuation exploiting differential moveout. *Geophysics* **30**, 348–362.

Shultz P.S. and Claerbout J.F. 1978. Velocity estimation and downward-continuation by wavefront synthesis. *Geophysics* **43**, 691–714.

Taner M.T. and Koehler F. 1969. Velocity spectra – digital computer derivation and applications of velocity functions. *Geophysics* **34**, 859–881.

Verschuur D. and Berkhout A. 1992. Surface-related multiple eliminations: Practical aspects. 62nd SEG Meeting, New Orleans, USA, Expanded Abstracts, 1100–1103.

Wiggins J. 1988. Attenuation of complex water-bottom multiples by wave equation-based prediction and subtraction. *Geophysics* **53**, 1527–1539.

Yilmaz O. 1989. Velocity stack processing. *Geophysical Prospecting* **37**, 357–382.

Zhou B. and Greenhalgh S. 1996. Multiple suppression by 2D filtering in the τ-p domain: a wave-equation-based method. *Geophysical Prospecting* **44**, 375–401.